Different Behavioral Types of Distributional Preferences Are Characterized by Distinct Neural Signatures

Katharina Koch[1*], Lorena R. R. Gianotti[1*], Jan Hausfeld[1,2], Mirjam Studler[1], and Daria Knoch[1]

Abstract

■ There are many situations where resources are distributed between two parties and where the deciding party has information about the initial distribution and can change its outcome, for example, the allocation of budget for funds or bonuses, where the deciding party might have self-interested motives. Although the neural underpinnings of distributional preferences of resources have been extensively studied, it remains unclear if there are different types of distributional preferences and if these types underlie different disposing neural signatures. We used source-localized resting EEG in combination with a data-driven clustering approach to participants' behavior in a distribution game in order to disentangle the neural sources of the different types of distributional preferences. Our findings revealed four behavioral types: Maximizing types always changed initial distributions to maximize their personal outcomes, and compliant types always left initial distributions unchanged. Disadvantage-averse types only changed initial distributions if they received less than the other party did, and equalizing types primarily changed initial distributions to fair distributions. These behavioral types differed regarding neural baseline activation in the right inferior frontal gyrus. Maximizing and compliant types showed the highest baseline activation, followed by disadvantage-averse types and equalizing types. Furthermore, maximizing types showed significantly higher baseline activation in the left orbitofrontal cortex compared to compliant types. Taken together, our findings show that different types of distributional preferences are characterized by distinct neural signatures, which further imply differences in underlying psychological processes in decision-making. ■

INTRODUCTION

The investigation of preferences for the distribution of resources has been of great interest in psychological and economic research (e.g., Cappelen, Hole, Sørensen, & Tungodden, 2007; Konow, 2003). There exists also extensive research on the neural underpinnings of distributional preferences (for recent meta-analysis, see Cutler & Campbell-Meiklejohn, 2019). However, previous research on the neural underpinnings of distributional preferences has primarily focused on task-dependent neural activity and the investigation of average behavior in distributional decisions. None of the previous studies has attempted to disentangle individual behavioral patterns and investigate the existence of different types of distributional preferences.

There are many situations in life where resources or tasks (e.g., food, money, land) are distributed between two parties. The deciding party often has strictly private information about the initial distribution and has the possibility to change its outcome. Initially, there can be three situations: Situations with disadvantageous, advantageous, and/or fair distributional outcomes for the deciding party. We investigated what the deciding party does in each of these situations. One can imagine that various behavioral types with distinct distributional preferences are possible. For example, some people may generally prefer to accept distributional outcomes independent of the initial situation, whereas others may generally prefer to maximize their personal outcomes, even if the initial situation already has a fair or advantageous outcome. Some people may prefer to change distributional outcomes to their favor in disadvantageous situations, but otherwise accept distributional outcomes in fair or advantageous situations. Finally, some people may prefer equal distributions in situations with either disadvantageous or advantageous outcomes, but accept distributional outcomes in fair situations.

Despite the fact that such behavioral types may affect life in society very differently, the psychological and neural mechanisms that underlie different types of distributional preferences remain largely unknown.

Previous research has shown that task-independent neural trait measurements, such as baseline neural activation and neuroanatomical measures of brain structure, allow inferences about the psychological processes that underlie individual differences in behavior (e.g., Gianotti, Dahinden, Baumgartner, & Knoch, 2019; Hahn et al., 2015; Watanabe et al., 2014; Baumgartner, Schiller, Hill, & Knoch, 2013; Studer, Pedroni, & Rieskamp, 2013; Morishima, Schunk, Bruhin, Ruff, & Fehr, 2012).

[1]University of Bern, Switzerland, [2]University of Amsterdam, Netherlands
*Both authors contributed equally to this work.

© 2021 Massachusetts Institute of Technology

Journal of Cognitive Neuroscience 33:10, pp. 2065–2078
https://doi.org/10.1162/jocn_a_01751

Downloaded from http://direct.mit.edu/jocn/article-pdf/33/10/2065/1962120/jocn_a_01751.pdf by guest on 18 October 2021

Here, we measure baseline neural activation with resting EEG. Resting EEG activity has previously demonstrated both high temporal stability (e.g., Cannon et al., 2012; Näpflin, Wildi, & Sarnthein, 2007; Dünki, Schmid, & Stassen, 2000) and high specificity (i.e., the extent to which a given EEG pattern uniquely belongs to a given person; e.g., Näpflin et al., 2007; Dünki et al., 2000). Longitudinal studies demonstrated temporal stability with test–retest reliabilities of up to 0.8 over a 5-year period and recognition rates of up to 99% over a 3-year period. Hence, neural traits measured with resting EEG are ideal to investigate differences between types of distributional preferences. Distinct types of distributional preferences might be further characterized by differences in decision-making processes. Eye-tracking is a widely used method to record and analyze decision-making processes by measuring the direction and duration of eye movements. Eye-tracking measures can reflect different cognitive and affective processes, such as subjective importance of inspected information, and also reveal differences in the search strategy, such as whether all information was looked at or heuristics were applied (for reviews, see Rahal & Fiedler, 2019; Orquin & Mueller Loose, 2013). Moreover, various eye-tracking measures have shown to reflect relevant processes in (social) decision-making tasks (e.g., Jiang, Potters, & Funaki, 2016; Fiedler, Glöckner, Nicklisch, & Dickert, 2013). The analysis of complementary data from process-tracing methods might therefore help to get a more complete understanding about differences between behavioral types and might further help to explain differences in underlying neural signatures.

The current research sought to answer the following questions: Can we identify distinct neural signatures underlying different behavioral types in distributional preferences? And, once identified, what do these signatures reveal about the psychological processes driving these different types of distributional preferences? To measure distributional preferences, we employed a distribution game during which the participants' eye movements were recorded. Participants played in the role of decision-makers and randomly chose one of five letters from A to E. The decision-makers were instructed to report the randomly drawn letter to an anonymous recipient. Each of the five letters was paired with a different distribution of points between both players. The decision-makers received either more (*advantageous situation*), less (*disadvantageous situation*), or an equal amount (*fair situation*) of points compared to the recipient. However, the decision-makers could report the randomly drawn letter as instructed, or report a different letter in order to change the distributional outcome to their preference. Note that these decisions had real monetary consequences for both players. Decision-makers underwent resting EEG recordings to investigate differences in neural signatures.

The following key elements in this study enabled us to answer our questions. First, we conducted a data-driven cluster analysis of the decisions made in the behavioral experiment to identify the full set of behavioral types that constitute the repertoire of distributional preferences among the participants. Second, we analyzed differences in baseline neural activation to identify underlying sources of these different types. Finally, eye-tracking recordings were analyzed to elaborate differences between the behavioral types and to complement findings from EEG analyses. Given that no previous studies tried to disentangle distinct types of distributional preferences, we conducted exploratory whole-brain-corrected analyses without any a priori hypotheses to identify distinct neural signatures.

METHODS

Participants

We initially wanted to collect data from as many individuals as possible within one academic year because of the cluster analysis approach. However, this study, which is part of a larger project, had to be terminated prematurely due to the COVID-19 pandemic. We stopped data acquisition shortly before a national state of emergency was announced and lockdown measures were enforced. Until then, we had recruited 65 students from the University of Bern for participation in this study in the role of decision-makers. One of these participants had to be excluded from the analyses because of technical problems. The mean age of the remaining 64 participants (14 male) was 21.3 years ($SD = 2.3$ years). All participants in the role of decision-makers were right-handed and reported no history of neurological or psychiatric disorders or alcohol and drug abuse. The study was approved by the local ethics committee (no. 2019-10-00007) and conducted according to the principles expressed in the Declaration of Helsinki. All participants gave written informed consent and were informed of their right to discontinue participation at any time. Participants were remunerated with 40 Swiss francs (CHF 40; CHF 1 ≈ USD 1), in addition to the money earned in the distribution game. The experiment was programmed in *z* tree (Fischbacher, 2007), and individuals were recruited via a Web-based Online Recruitment System (ORSEE) (Greiner, 2015). The study procedures were carried out in one session, which encompassed the behavioral experiment, eye tracking recordings, and resting EEG recordings. After the behavioral experiment, participants completed various questionnaires, including a handedness questionnaire (Chapman & Chapman, 1987), the lay rationalism questionnaire (Hsee, Yang, Zheng, & Wang, 2015), the Guilt–Negative–Behavior–Evaluation and the Guilt–Repair subscales of the Guilt and Shame Proneness scale (Cohen, Wolf, Panter, & Insko, 2011), and the Honesty–Humility subscale of the HEXACO personality framework (Ashton & Lee, 2007). The Honesty–Humility subscale is a 10-item questionnaire that measures participants' level of fairness, sincerity, greed avoidance, and modesty on a 5-point Likert scale. All questionnaires were filled out online using Qualtrics.

Downloaded from http://direct.mit.edu/jocn/article-pdf/33/10/2065/1962120/jocn_a_01751.pdf by guest on 18 October 2021

Distribution Game

The behavioral experiment took place at a behavioral laboratory with interconnected computer terminals. At the beginning of each experimental session, participants were randomly assigned to cubicles where they made their decisions anonymously. They were not allowed to talk to each other. Participants played eight trials of a modified version of the distribution game by Barron, Stüber, and van Veldhuizen (2019) in the role of decision-makers, where they interacted with anonymous recipients during the experiment. Notably, the recipients were present in the laboratory, had a passive role in the distribution game, and were paid according to the decisions of the decision-makers at the end of the experiment (see below). As illustrated in Figure 1, in each trial, the decision-makers were instructed to draw randomly a letter from A to E. After the random draw, the five letters were displayed on the next screen. Each letter was associated with a different distribution of 10 points (1 point = 1 CHF) between decision-makers and recipients. Decision-makers drew distributions where they received either 1, 3, 5, 7, or 9 points. The remainder of the 10 points went to the recipient. The decision-makers could decide either to report the drawn letter as instructed or to report a different letter in order to receive a different amount of points. The distribution game consisted of eight trials, and all decision-makers drew the same distributions of points: There were four disadvantageous situations, two advantageous situations, and two fair situations. In *disadvantageous situations*, the decision-maker drew a distribution where they received fewer points than the recipient did (1 or 3 points). In *advantageous situations*, the decision-maker drew a distribution where they received more points than the recipient did (7 or 9 points). In *fair situations*, the decision-maker drew a distribution where they received as many points as the recipient did (5 points). To avoid habituation effects in the eye-tracking recordings, the distributions were displayed in different order in each trial, and each distribution was paired with a different letter. There was no time constraint for making a decision. On average, participants needed 2.90 min (SD = 0.55 min) to complete all eight trials of the paradigm. Three control questions before the distribution game ensured participants' understanding (e.g., "Which reported letter would give you the highest amount of points?"). Participants could only proceed to the next control question after giving the correct answer. After the control questions, participants completed two exercise trials. On average, participants needed 2.59 min (SD = 0.43 min) to complete the control questions and exercise trials. After the distribution game, two questions were asked to assess task difficulty using a 5-point Likert scale ("It was difficult to remember the drawn letters"; "I tried to remember the drawn letters") and one more question was asked to ensure the understanding of the paradigm using a dichotomous answer format (yes/no; "Were you aware that you did not have to report the drawn letters?"). Participants in the role of the decision-maker were informed in advance that, at the end of the study, their distribution of a randomly chosen trial was implemented, resulting in the respective points for them and the recipient. The recipients did not make any decisions with effect on the study outcome and did not participate in EEG recordings.

As established previously, we have adapted the paradigm of Barron et al. (2019) for the purpose of our study. In the original paradigm, participants drew numbers that corresponded to a personal payout in a first step and decided which number to report in a second step. The instruction to draw letters instead of numbers is part of our adaptation. One disadvantage of tasks where a number is drawn in a first step and then mapped to earnings is that there is "a natural and common measure of the distance between observed outcomes and reports" (Gneezy, Kajackaite, & Sobel, 2018). This might be especially crucial for people who care about how large the change from initial to chosen outcome is. In our task, we randomly map the letter to payoff, which should help to

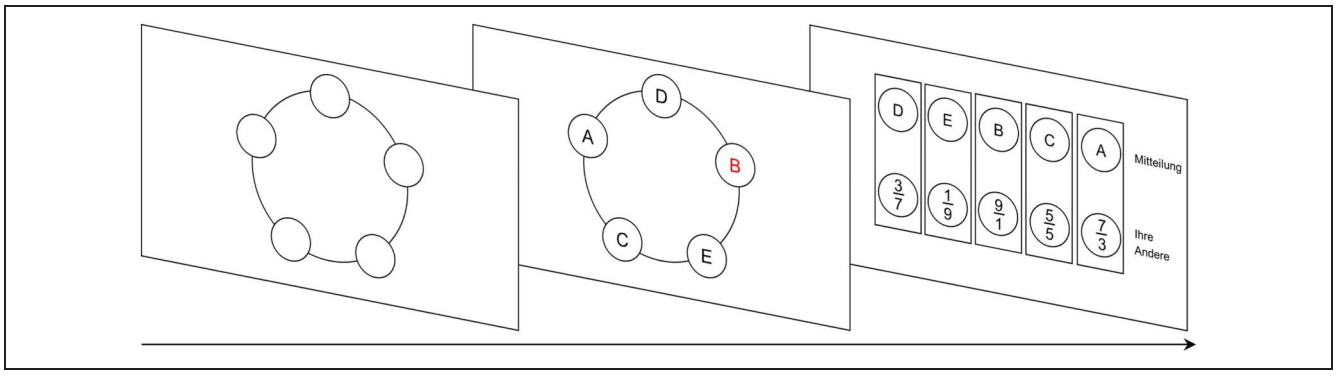

Figure 1. Illustration of a trial in the distribution game. The decision-makers click on one of the five blank circles on the first screen to draw a random letter from A to E. After clicking, the letters appear within the circles on the second screen, and the drawn circle is highlighted. The third screen displays all letters with the associated distributions of points between the decision-makers and the recipients. Decision-makers have to decide whether to report the drawn letter as instructed or to report a different letter that corresponds to a different distribution of points.

Downloaded from http://direct.mit.edu/jocn/article-pdf/33/10/2065/1962120/jocn_a_01751.pdf by guest on 18 October 2021

disturb the natural and common distance. For example, drawing a "1" and then choosing a "5," is likely to be perceived different than drawing a "C" and then reporting a "5" or "E." A second benefit of our adaptation is that it makes eye-tracking recordings feasible: In the first step, participants click on a tile and learn the letter. The second step contains the whole decision process, that is, finding the already drawn and learned letter and learning about the outcome. Thus, the time spent on the third screen includes the learning of the value and finding a preferred outcome. Participants were not explicitly instructed about the reason why they had to draw letters (as in Barron et al., 2019).

Eye Tracking Recording and Processing

Eye movements were recorded with Tobii 4C eye tracking devices at a sampling rate of 90 Hz. Participants sat approximately 62 cm in front of their screens, which were 21.5 in. in size and had a resolution of 1920 × 1080 pixels. These eye-trackers do not allow a calibration above 1.5°. Gaze data were clustered into fixations with the Density-Based Spatial Clustering of Applications with Noise (DBSCAN) algorithm (Hahsler, Piekenbrock, & Doran, 2019). A fixation was defined as a cluster of single measurements appearing within a minimum time of 50 msec and a 50-pixel threshold for the distance between points. Letters were displayed in the upper half of the screen and distributions in the lower half of the screen. Circular areas of interest (AOIs) were defined by a 100-pixel radius from the center of each letter and each distribution, resulting in 10 nonoverlapping AOIs. Fixations outside AOIs were not considered for analyses. Information during decisions were presented with a large enough distance between AOIs to not misidentify gaze on a wrong AOI (Orquin, Ashby, & Clarke, 2016).

EEG Recording and Processing

For the recording of resting EEG, participants were seated in a cubicle shielding from visual distractions in a quiet and dimly lit room with the experimenter. They were instructed that the EEG recording would be conducted while they rested with their eyes alternately opened or closed. The resting EEG protocol consisted of the participants resting for 20 sec with their eyes opened, followed by 40 sec with their eyes closed. This was repeated 5 times. Such a protocol guarantees minimal fluctuations in participants' vigilance state. The experimenter gave the instructions about eyes opening and closing. In line with previous neural trait studies (e.g., Li et al., 2017; Baumgartner, Gianotti, & Knoch, 2013; Kam, Bolbecker, O'Donnell, Hetrick, & Brenner, 2013; Vecchio et al., 2013; Gianotti et al., 2009), data analyses were based on the 200 sec eyes-closed condition.

Resting EEG was continuously recorded using 59 active electrodes (Brain Products, actiCAP) mounted in an elastic cap and placed according to the international 10–10 system (Nuwer et al., 1998), at a sampling rate of 500 Hz (third-order low-pass filter at 131 Hz). The electrode at the position FCz was the recording reference, and the electrode at the position CPz served as ground. Horizontal and vertical eye movements were recorded with electrodes at the left and right outer canthi and at the right infraorbital area. Impedances were kept below 25 kΩ. After an automatic artifact rejection (maximal allowed voltage step: 15 μV; maximal allowed amplitude: ± 100 μV; minimal allowed activity in intervals of 100 msec: 0.5 μV), data were visually inspected to eliminate residual artifacts. The data were then recomputed against the average reference. All artifact-free 2-sec epochs were extracted. On average, 87.1 epochs (SD = 16.7 epochs) per participant were available. A fast Fourier Transformation (using a square window) was applied to each epoch and channel to compute the power spectra with 0.5-Hz resolution. The spectra for each channel were averaged over all epochs for each participant. Absolute power values were integrated for the following seven independent frequency bands (Kubicki, Herrmann, Fichte, & Freund, 1979): delta (1.5–6 Hz), theta (6.5–8 Hz), alpha1 (8.5–10 Hz), alpha2 (10.5–12 Hz), beta1 (12.5–18 Hz), beta2 (18.5–21 Hz), and beta3 (21.5–30 Hz).

Standardized low-resolution electromagnetic tomography (sLORETA; Pascual-Marqui, 2002) was used to estimate the intracerebral electrical sources that generated the scalp-recorded activity at each of the EEG frequency bands. The sLORETA method is a properly standardized, discrete, 3-D distributed, linear, minimum norm inverse solution that allows for localization of the intracerebral sources of scalp-recorded electromagnetic signals. The particular form of standardization used in sLORETA endows the tomography with the property of exact localization to test point sources, and thereby yields images of standardized current density with exact localization, albeit with low spatial resolution (i.e., neighboring neural sources will be highly correlated). sLORETA has been validated in several simultaneous EEG/fMRI studies (Mobascher, Brinkmeyer, Warbrick, Musso, Wittsack, Saleh, et al., 2009a; Mobascher, Brinkmeyer, Warbrick, Musso, Wittsack, Stoermer, et al., 2009b) and in an EEG localization study for epilepsy (Rullmann et al., 2009). In the current implementation of sLORETA, computations are conducted in a realistic head model using the MNI152 template (Mazziotta et al., 2001), with the 3-D solution space restricted to cortical gray matter, as determined by the probabilistic Talairach atlas (Lancaster et al., 2000). The intracerebral volume is partitioned in 6239 voxels at 5-mm spatial resolution. Thus, sLORETA images represent the standardized electric activity at each voxel in neuroanatomic Montreal Neurological Institute (MNI) space as the exact magnitude of the estimated current density. Using the manual regularization method in the sLORETA software, we selected the transformation matrix with the signal-to-noise ratio set to 10. To reduce confounds that have no regional specificity, for each participant,

Downloaded from http://direct.mit.edu/jocn/article-pdf/33/10/2065/1962120/jocn_a_01751.pdf by guest on 18 October 2021

sLORETA images were normalized to a total power of one and then log-transformed before statistical analyses.

Statistical Analyses

The first goal of this study was to classify individual behavioral data into meaningful behavioral types to disentangle differences and similarities among individuals in their preferences for the distribution of resources across different situations. To achieve this goal, we applied a *k*-means cluster analysis. The mean difference between the reported and the initial distributions was calculated for each of the three situations in the distribution game (*disadvantageous, advantageous,* and *fair* situations), resulting in three difference scores. These three scores were used as input variables in the cluster analysis. The gap statistic method (Tibshirani, Walther, & Hastie, 2001) was used to determine the number of clusters, which calculates the difference or gap of within-cluster variance according to a given cluster number and the expected variance given a null distribution. The number of clusters that maximize the gap statistic are considered the optimal number of clusters for a data set.

The second and main goal of this study was to examine the neural signatures of the different behavioral types. For that purpose, we conducted whole-brain-corrected ANOVAs in the seven frequency bands separately to compare the neural baseline activations of the behavioral types that had emerged. Because ANOVAs are not implemented in the sLORETA software, normalized and log-transformed current density values for each voxel and participants were exported from sLORETA to MATLAB (The MathWorks Inc.). ANOVAs were then performed on each voxel using the *anova1* function in MATLAB and specifying the between-subjects factor with four levels (four behavioral types). The corrections for multiple testing were incorporated using the nonparametric permutation tests described in Nichols and Holmes (2002). In detail, 5000 permutations were run in order to estimate the empirical probability distributions. The statistical F-images were then thresholded at the corresponding critical probability threshold (corrected for multiple comparisons at $p < .05$), and voxels with statistical values exceeding this threshold have their null hypotheses rejected. For regions that displayed significant, whole-brain-corrected differences between the behavioral types, the respective voxel with the strongest effect was used as the center for spherical ROIs (radius: 10 mm). Averaged current density values were extracted for all voxels within these ROIs for visualization and further analyses.

Finally, we analyzed eye-tracking data to elaborate similarities and differences between the behavioral types and complement findings from EEG analyses. To explore differences in the stability of decision-making processes, we calculated the standard deviation of the total number fixations made during the distribution game for each individual and used it in a one-way ANOVA with the behavioral types as between-subjects factor. In addition, we used the proportion of fixations on the distributions, that is, the number of fixations on distributions divided by the total number of fixations on either distributions or letters. This proportion serves as an indicator for relative importance of the inspected objects (e.g., Poole, Ball, & Phillips, 2005; Jacob & Karn, 2003). A value of 0 indicates that all fixations were made on the letters, whereas a value of 1 indicates that all fixations were made on the distributions. We used unpaired *t* tests to examine differences in the proportion measure between the behavioral types.

RESULTS

Emergence of Four Behavioral Types

As indicated by gap statistics, *k*-means cluster analysis revealed a solution with four separate clusters (see Figure 2), using the average difference between the reported and the initial distributions in disadvantageous, advantageous, and fair situations as input variables.

The first cluster included 17.2% of the sample ($n = 11$; *equalizing type*), who changed the distributional outcome to their favor in disadvantageous situations (*mean* difference score ± *SD*: 2.64 ± 0.71 points) and to the recipient's favor in advantageous situations (*mean* difference score ± *SD*: −2.82 ± 1.17 points), and accepted the given distributions in fair situations (*mean* difference score ± *SD*: 0.45 ± 1.13 points). The second cluster included 20.3% of the sample ($n = 13$; *maximizing type*). Almost all participants of this type reported to have drawn the highest number of points in every trial of the distribution game (*mean* difference score ± *SD* in disadvantageous situations: 6.81 ± 0.48 points, advantageous situations: 0.54 ± 1.13 points, fair situations: 4.00 ± 0.00 points). The third cluster included 28.1% of the sample ($n = 18$; *compliant type*), who left almost every distribution unchanged in the distribution game (*mean* difference score ± *SD* in disadvantageous situations: 0.97 ± 0.98 points, advantageous situations: 0.00 ± 0.00 points, fair situations: 0.33 ± 1.08 points). The fourth cluster included 34.4% of the sample ($n = 22$; *disadvantage-averse type*) who changed the distributional outcome to their favor in disadvantageous situations (*mean* difference score ± *SD*: 4.61 ± 1.32 points) but accepted the majority of distributions in fair (*mean* difference score ± *SD*: 0.23 ± 0.53 points) and advantageous situations (*mean* difference score ± *SD*: −0.09 ± 0.43 points).

Pearson's chi-square tests with Yates' continuity correction demonstrated no significant differences in the sex ratio between the four behavioral types, $\chi^2(3) = 3.32$, $p = .35$. The four behavioral types did not differ in age (ANOVA, $F(3, 61) = 0.75$, $p = .52$), handedness (ANOVA, $F(3, 61) = 0.67$, $p = .58$), personality traits of honesty and humility (ANOVAs: all $F(3, 57) \leq 1.21$, $p \geq .32$), nor in the two subscales of the Guilt and Shame Proneness scale (ANOVAs, both $F(3, 57) \leq 1.86$, $p \geq$

Downloaded from http://direct.mit.edu/jocn/article-pdf/33/10/2065/1962120/jocn_a_01751.pdf by guest on 18 October 2021

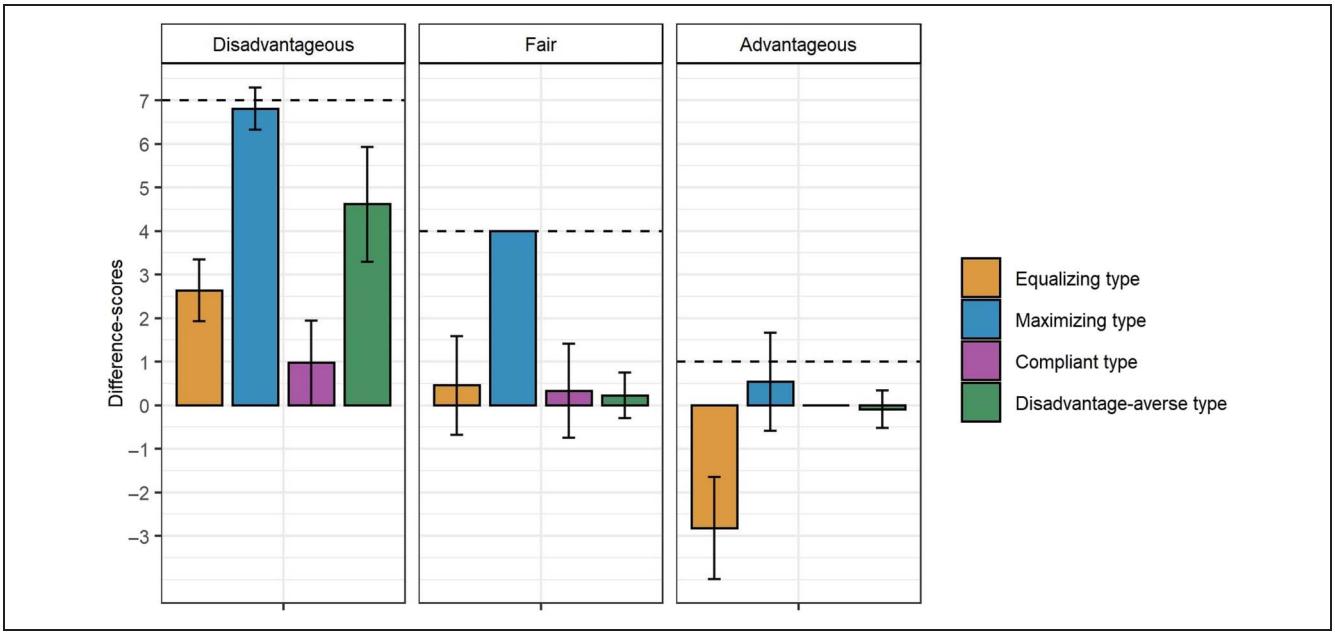

Figure 2. The decision-makers' average behavior in the distribution game per behavioral type, illustrated with the average difference between the reported and the initial distributions (difference scores). Depicted is the average difference in points (± *SD*) in the disadvantageous, fair, and advantageous situations: equalizing type (yellow), maximizing type (blue), compliant type (purple), and disadvantage-averse type (green). The black horizontal dotted lines represent the maximal possible difference in each of the situations. A difference of zero indicates that the initial distribution was reported, that is, participants accepted the given distributional outcome and have not used the possibility of redistribution.

.15). There was an almost significant difference between the behavioral types in lay notion of rationality (ANOVA, $F(3, 60) = 2.62, p = .059, \omega^2 = 0.07$). Post hoc unpaired *t* test demonstrated that the maximizing type has higher lay notion of rationality (*mean* = 27.77; *SD* = 6.18), that is, the notion of using reason rather than feelings, compared to the compliant type (*mean* = 22.61, *SD* = 4.34, $t(29) = 2.74$, $p = .011$, Cohen's $d = 1.00$), the disadvantage-averse type (*mean* = 24.27, *SD* = 4.93, $t(33) = 1.85, p = .074$, Cohen's $d = 0.65$), and the equalizing type (*mean* = 23.55, *SD* = 5.82, $t(22) = 1.71, p = .101$, Cohen's $d = 0.70$). No differences were found between the remaining groups (*t* tests, all $t \leq 1.12, p \geq 0.271$). Notably, participants with higher lay notion of rationality, as evidenced by the maximizing type, earned more money in the experiment. Specifically, unpaired *t* tests revealed that the maximizing type made significantly more money (CHF; *mean* = 70.3, *SD* = 4.1) compared to the equalizing type (*mean* = 39.8, *SD* = 4.1, $t(22) = 18.14, p < .001$, Cohen's $d = 7.43$), the compliant type (*mean* = 38.6, *SD* = 4.7, $t(29) = 19.49$, $p < .001$ Cohen's $d = 7.09$), and the disadvantage-averse type (*mean* = 52.7, *SD* = 5.4, $t(33) = 10.19$, $p < .001$ Cohen's $d = 3.56$).

As shown in Table 1, the behavioral types differed regarding consistency in the display of distributional preferences across situations. More specifically, equalizing types showed preferences for fair distributions in 58 of all 88 decisions (65.9%), but also showed a considerable amount of behavioral variability in disadvantageous, advantageous, and fair situations. In disadvantageous situations, they changed initial distributions to advantageous distributions in 7 of 44 decisions (15.9%) and left them unchanged in 11 of 44 decisions (25.0%). In advantageous situations, they changed initial distributions to disadvantageous distributions in 2 of 22 decisions (9.1%) and left them unchanged in 5 of 22 decisions (22.7%). In fair situations, they changed initial distributions to disadvantageous distributions in 1 of 22 decisions (4.5%) and changed them to advantageous distributions in 4 of 22 decisions (18.2%).

Maximizing types showed highly consistent behavior across the three situations by reporting the most advantageous distribution in 97 of all 104 decisions (93.3%). Compliant types were also characterized by highly consistent behavior across the three situations and left the initial distributions unchanged in 117 of all 144 decisions (81.3%).

Finally, disadvantage-averse types showed high consistency in the display of distributional preferences in fair and advantageous situations, reporting the initial distributions in 80 of 88 decisions (90.9%), but low consistency in the display of distributional preferences in disadvantageous situations. In these situations, they changed the initial distributions to fair distributions in 30 of 88 decisions (34.1%), changed them to advantageous distributions in 48 of 88 decisions (54.6%), and left them unchanged in 10 of 88 decisions (11.4%).

Neural Signatures of the Four Behavioral Types

Our exploratory whole-brain-corrected source localization analyses revealed significant differences between the four

Downloaded from http://direct.mit.edu/jocn/article-pdf/33/10/2065/1962120/jocn_a_01751.pdf by guest on 18 October 2021

Table 1. Contingency Table Reporting the Frequency of Different Initial and Reported Distributions per Behavioral Type

			Reported Distribution					
			Disadvantageous		*Fair*	*Advantageous*		*Total*
Behavioral Type	*Initial Distribution*		*1:9*	*3:7*	*5:5*	*7:3*	*9:1*	*Decisions*
Equalizing type (n = 11)	Disadvantageous	1:9	5	0	12	4	1	22
		3:7	1	5	14	1	1	22
	Fair	5:5	0	1	17	2	2	22
	Advantageous	7:3	1	0	5	5	0	11
		9:1	0	1	10	0	0	11
Maximizing type (n = 13)	Disadvantageous	1:9	0	0	1	1	24	26
		3:7	0	0	0	2	24	26
	Fair	5:5	0	0	0	0	26	26
	Advantageous	7:3	1	0	0	2	10	13
		9:1	0	0	0	0	13	13
Compliant type (n = 18)	Disadvantageous	1:9	24	2	7	0	3	36
		3:7	1	28	6	1	0	36
	Fair	5:5	0	1	31	1	3	36
	Advantageous	7:3	0	0	0	17	1	18
		9:1	0	0	0	1	17	18
Disadvantage-averse type (n = 22)	Disadvantageous	1:9	2	0	14	5	23	44
		3:7	0	8	16	8	12	44
	Fair	5:5	0	0	40	3	1	44
	Advantageous	7:3	0	0	0	21	1	22
		9:1	0	0	0	3	19	22

Note that differences in number of total decisions are because of different number of participants per behavioral type and because of different number of disadvantageous, advantageous, and fair decisions. There were four decisions with disadvantageous, two decisions with advantageous, and two decisions with fair initial distributions per participant.

behavioral types in one specific cluster in the right inferior frontal gyrus (IFG) in the alpha1 frequency band (MNI coordinate peak voxel: $x = 50, y = 6, z = 31$, Brodmann's area 9; ANOVAs, all voxels: $F(3, 60) > 5.89, p < .05$, $\omega^2 > 0.28$, whole-brain-corrected; Figure 3A). As shown in Figure 3B, post hoc unpaired comparisons revealed that the equalizing type showed higher alpha1 current density in the right IFG compared to the maximizing type (t test, $t(22) = 4.13, p < .001$, Cohen's $d = 1.69$), the compliant type (t test, $t(27) = 3.21, p = .003$, Cohen's $d = 1.23$), and the disadvantage-averse type (t test, $t(31) = 2.32, p = .027$, Cohen's $d = 0.86$). Moreover, the maximizing type showed lower alpha1 current density in the right IFG compared to the disadvantage-averse type (t test, $t(33) = 3.28$, $p = .002$, Cohen's $d = 1.15$), but no significant differences compared to the compliant type (t test, $t(29) = 1.15, p = .259$). Finally, a trend was also found between the compliant type and the disadvantage-averse type (t test, $t(38) = 1.89, p = .074$, Cohen's $d = 0.58$).

Interestingly, though, despite very different distributional preferences, the maximizing type and compliant type did not differ regarding their baseline activation in the right IFG. Analysis of eye tracking data showed significant differences in the stability of looking patterns, measured with the standard deviation of the number fixations made over all eight trials (ANOVA, $F(3, 59) = 3.71$, $p = .016$, $\omega^2 = 0.11$). As shown in Figure 4, post hoc comparisons revealed that the maximizing type and compliant type show similar stability in looking patterns (t test, $t(28) = -0.03$, $p = .977$). In contrast, the disadvantage-averse type shows significantly lower stability in looking patterns (i.e., higher standard deviation) compared to the maximizing type (t test, $t(33) = -2.57$, $p = .015$, Cohen's $d = 0.90$) and the compliant type (t test, $t(37) = -2.82, p = .008$, Cohen's $d = 0.91$), but not compared to the equalizing type (t test, $t(31) = -0.41, p = .687$). For the equalizing type, a trend toward lower stability in looking patterns was found compared to the

Downloaded from http://direct.mit.edu/jocn/article-pdf/33/10/2065/1962120/jocn_a_01751.pdf by guest on 18 October 2021

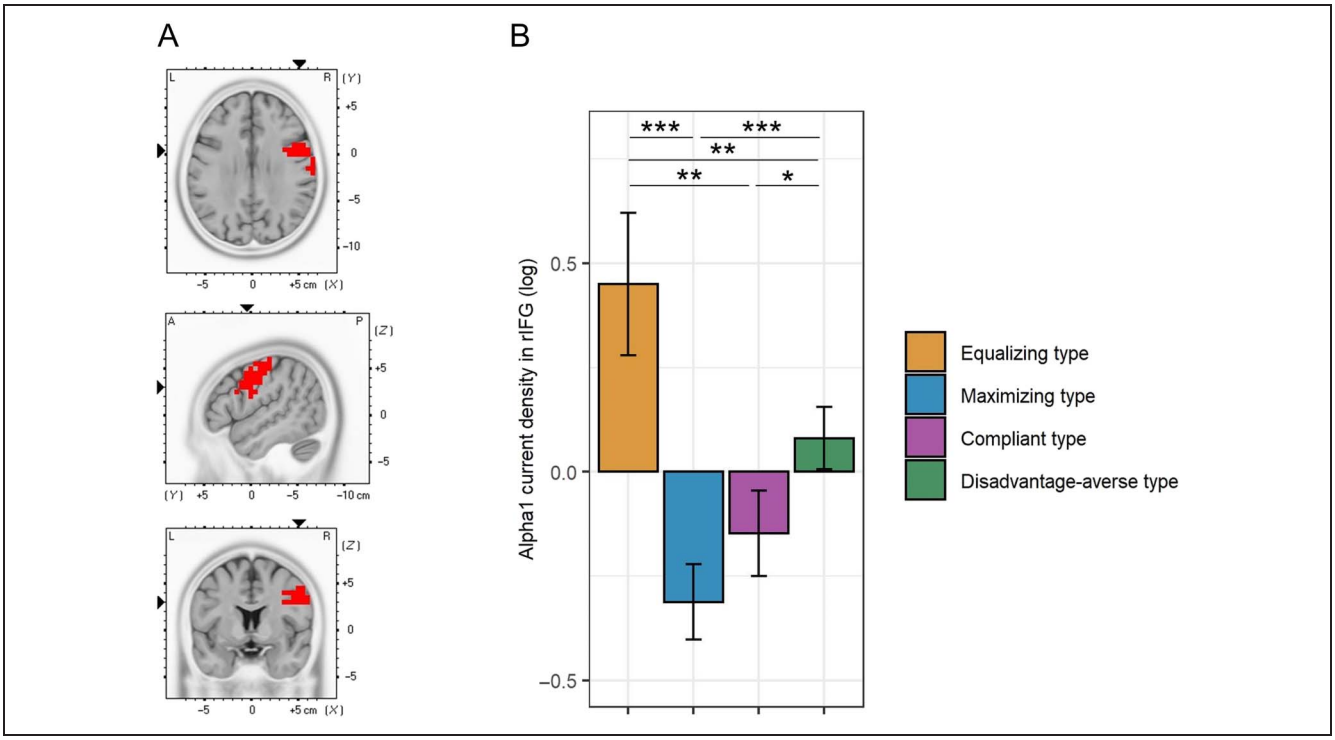

Figure 3. Region of the right Inferior Frontal Gyrus (rIFG) showing differences in baseline EEG alpha1 current density (A/m2) between the four behavioral types. On A, locations of the voxels that showed significant differences (whole-brain-corrected) are indicated in red ($p < .05$). On B, the bar graph (based on a 10-mm spherical ROI around the peak depicted on A) illustrates differences in baseline alpha1 current density between the four behavioral types: equalizing type (yellow), maximizing type (blue), compliant type (purple), and disadvantage-averse type (green). Error bars correspond to standard errors of the means. The asterisks denote the significance level of the post hoc unpaired *t* test (***: $p < .001$; **: $.001 < p < .05$; *: $.05 < p < .10$).

compliant type (*t* test, $t(26) = 1.83$, $p = .079$, Cohen's $d = 0.71$), and a weak trend toward significance was found compared to the maximizing type (*t* test, $t(22) = 1.69$, $p = .105$, Cohen's $d = 0.69$).

Although the maximizing and compliant type show striking differences in their distributional preferences, they show similar stability of looking patterns and similar baseline activity in the right IFG. How might these two behavioral types differ, then? Because of their striking behavioral differences, there must be manifest differences in baseline activity in other brain regions and/or other frequency bands. For this purpose, the maximizing and compliant type were entered in further exploratory analyses. As shown in Figure 5, findings reveal that the maximizing type shows lower alpha1 current density in the left OFC compared to the compliant type (MNI coordinate peak voxel: $x = -15$, $y = 55$, $z = -20$, Brodmann's area 11; ANOVAs, all voxels: $F(1, 29) > 12.7$, $p < .05$, $\omega^2 > 0.26$, whole-brain-corrected).

Eye tracking results complement the finding that the maximizing and compliant type differ in baseline activity in the left OFC. As shown in Figure 6, the proportions of fixations on distributions indicate that both behavioral types weigh the value of the letters and distributions differently. The unpaired *t* test revealed that the maximizing type is characterized by significantly higher proportions

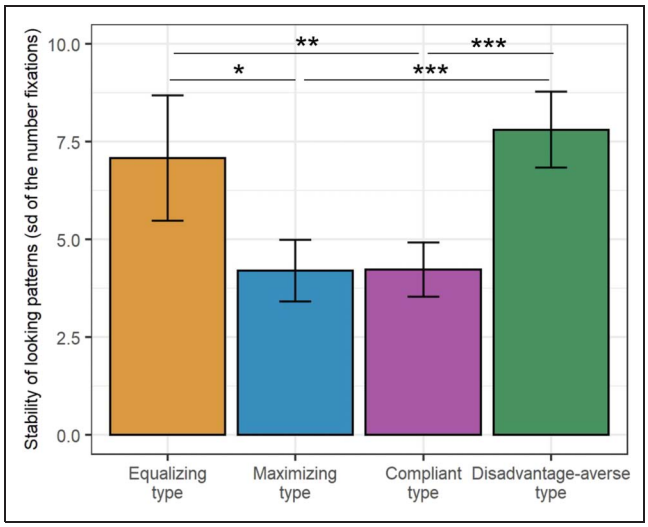

Figure 4. Differences in stability of looking patterns between the four behavioral types: equalizing type (yellow), maximizing type (blue), compliant type (purple), and disadvantage-averse type (green). Stability was calculated using the standard deviation of the number fixations made during the eight trials of the distribution game. Higher values indicate lower stability of looking patterns. Error bars correspond to standard errors of the means. The asterisks denote the significance level of the post hoc unpaired *t* test (*** $.001 < p < .05$; **: $.05 < p < .1$, *: $p = .105$).

Downloaded from http://direct.mit.edu/jocn/article-pdf/33/10/2065/1962120/jocn_a_01751.pdf by guest on 18 October 2021

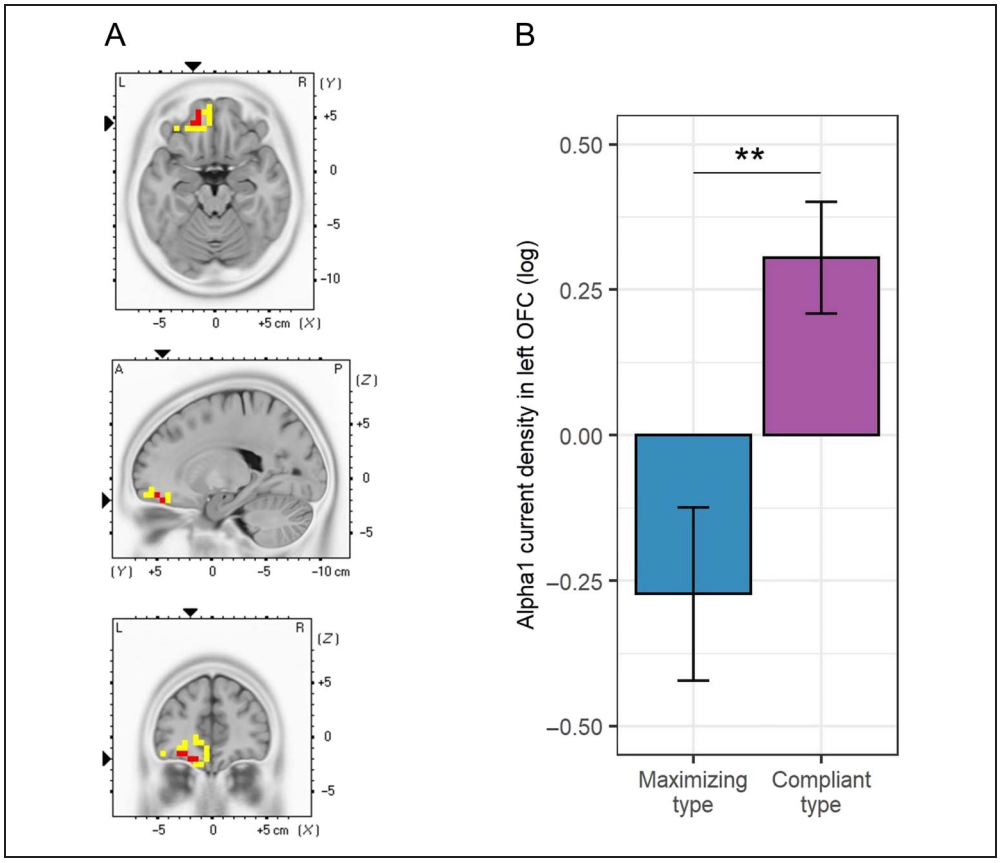

Figure 5. Region of the left OFC showing differences in baseline EEG alpha1 current density (A/m2) between the maximizing and the compliant type. On A, locations of the voxels that showed significant differences (whole-brain-corrected) are indicated in red ($p < .05$) and in yellow ($p < .10$). On B, the bar graph (based on a 10-mm spherical ROI around the peak depicted on the A) illustrates the baseline alpha1 current density differences between the maximizing type (blue) and the compliant type (purple). Error bars correspond to standard errors of the means. The asterisks denote the significance level of the post hoc unpaired t test (**$p < .05$).

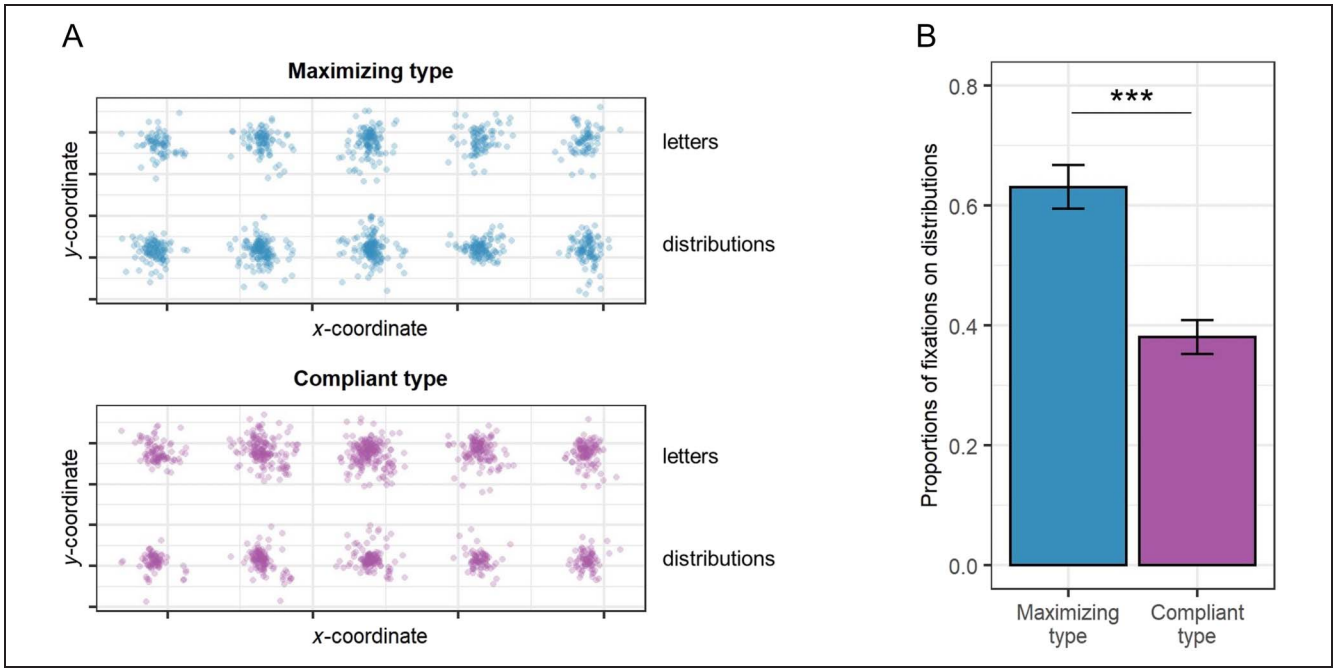

Figure 6. Fixations and proportions of fixations of the maximizing type (blue) and compliant type (purple). A displays the fixation patterns (i.e., every circle corresponds to one fixation) on letters and distributions, separately for the maximizing and the compliant type. x and y coordinates correspond to the screen position in pixels. Fixations on the upper half of the screen correspond to fixations on letters, and fixations on the lower half of the screen correspond to fixations on distributions. B displays differences in the proportions of fixations on distributions. Proportions of fixations on distributions were calculated with the number fixations made on the distributions divided by the number of fixations made on the distributions and letters during the distribution game. Error bars correspond to standard errors of the means. The asterisks denote the significance level of the unpaired t test (***$p < .001$).

Downloaded from http://direct.mit.edu/jocn/article-pdf/33/10/2065/1962120/jocn_a_01751.pdf by guest on 18 October 2021

of fixations on distributions compared to the compliant type, $t(28) = 5.48$, $p < .001$, Cohen's $d = 2.02$. In other words, the maximizing type looks primarily at distributions (*mean* = 0.63, *SD* = 0.13), whereas the compliant type primarily inspects letters (*mean* = 0.38, *SD* = 0.12) in the distribution game.

DISCUSSION

Although different types of distributional preferences clearly have a divergent social impact, the sources of their heterogeneity are poorly understood. We used source-localized resting EEG in combination with a model-free clustering approach of participants' behavior in a distribution game to explain this heterogeneity. The cluster analysis identified four distinct behavioral types of distributional preferences. A percentage of 20.3 of our sample shows preferences for the maximization of distributional outcomes (*maximizing type*), and 34.4% of our sample shows aversion to disadvantageous, but not to fair or advantageous distributional outcomes (*disadvantage-averse type*). A percentage of 28.1 of our sample shows strong preferences to accept distributional outcomes irrespective the situation (*compliant type*). Finally, 17.2% of our sample shows preferences for fair distributions in both advantageous and disadvantageous situations and accepts the distributional outcome in fair situations (*equalizing type*).

By analyzing task-independent neural baseline activation, we were able to clearly differentiate and characterize the four identified behavioral types and shed light on possible underlying psychological mechanisms. Our findings revealed that the maximizing type and the compliant type are characterized by lower task-independent alpha1 current density in the right IFG compared to the equalizing type and the disadvantage-averse type. Moreover, the equalizing type is characterized by higher task-independent alpha1 current density in the same area compared to the disadvantage-averse type. Interestingly, the maximizing and compliant type show no significant differences in task-independent current density in the right IFG, despite the fact that they displayed very different distributional preferences in the distribution game. As baseline current density in the alpha band is an inverse indicator for cortical activation (Oakes et al., 2004; Shagass, 1972), these findings suggest that the maximizing and the compliant type are characterized by the highest activation of the right IFG, followed by the disadvantage-averse type. The equalizing type is characterized by the lowest activation of the right IFG. It is important to note that these findings are based on whole-brain-corrected analyses.

These findings might be related to the role of the right IFG in the resolution of interferences (for meta-analysis, see Zhang, Geng, & Lee, 2017). Specifically, it has been shown that the right IFG is engaged in the resolution of interferences from distractors (e.g., van Velzen, Vriend, de Wit, & van den Heuvel, 2014; Armbruster, Ueltzhöffer, Basten, & Fiebach, 2012; Nee, Wager, & Jonides, 2007; Liu, Banich, Jacobson, & Tanabe, 2004). The displayed letters and distributions in the distribution game might cause some interference or distraction because they pose alternative response options to the initial distribution. Maximizing types show highly consistent and distractor-resistant behavior across the three situations in the distribution game, and report the distribution with the most advantageous outcome for them in almost all trials of the distribution game (93.3% of their decisions; see Table 1 for details). Compliant types also show relatively consistent and distractor-resistant behavior, and reported the initial distributions in almost all trials of the distribution game (81.3% of their decisions). This distractor-resistant behavior might be related to their higher baseline activation in the right IFG, or in other words, because of higher capacity to resolve interferences by focusing on the response option corresponding to their distributional preference irrespective the situation.

In contrast to maximizing and compliant types, disadvantage-averse types were less consistent in their behavior and therefore less resistant to distractions caused by multiple response alternatives in disadvantageous situations. More specifically, if disadvantage-averse types drew disadvantageous distributions, they left the initial distributions either unchanged (11.4% of decisions in disadvantageous situations), changed them to advantageous distributions (54.6% of decisions in disadvantageous situations), or changed them to fair distributions (34.1% of decisions in disadvantageous situations). In fair or advantageous situations, however, disadvantage-averse types primarily left the initial distributions unchanged (90.9% of decisions in fair situations and in advantageous situations). Regarding interference resolution, we speculate that disadvantage-averse types might perceive interference or get distracted by the alternative response options in disadvantageous situations because the initial distributions do not correspond to the participants' distributional preference. The initial distributions in advantageous or fair situations, on the other hand, might already be in line with the distributional preferences of disadvantage-averse types. Hence, the response alternatives might not cause any interferences or distractions in advantageous or fair situations. This variability of behavior across different situations might be reflected by lower baseline activation in the right IFG in the disadvantage-averse type, which might in turn reflect lower capacity for distractor-resistant behavior. Moreover, we found a trend toward significantly different baseline activation in the right IFG between the compliant and disadvantage-averse type. This trend might be related to similar behavioral patterns in fair and advantageous situations, which make up half of the played trials in the distribution game. Neither the compliant nor the disadvantage-averse type show strong preferences to change distributional outcomes in these situations.

Finally, equalizing types were also less consistent in their behavior and therefore less resistant to distractions caused

Downloaded from http://direct.mit.edu/jocn/article-pdf/33/10/2065/1962120/jocn_a_01751.pdf by guest on 18 October 2021

by multiple response alternatives in the distribution game. Although they showed preferences for fair distributional outcomes (65.9% of their decisions), there was also a considerable amount of variability in the decisions of equalizing types, where the initial distributions were left unchanged (25.0% of decisions in disadvantageous situations, 22.7% in advantageous situations) or where initial distributions were changed to advantageous distributions (15.9% of decisions in disadvantageous situations, 18.2% of decisions in fair situations). Regarding interference resolution, we speculate that equalizing types might perceive interference or get distracted by the alternative response options in all three situations of the distribution game. This behavioral variability across situations might be reflected by lower baseline activation in the right IFG compared to the other behavioral types, which might in turn be related to lower capacity for distractor-resistant behavior.

Taken together, these findings show that participants who behaved consistently across different situations in the distribution game show higher baseline activation in the right IFG. Conversely, participants who adapted their behavior across situations in the distribution game show reduced baseline activation in the right IFG.

The stability of looking patterns across situations, measured with eye-tracking devices, supports these findings. The maximizing and the compliant type showed higher stability in looking patterns compared to the other two types. This implies that the looking patterns of the maximizing and compliant type are less susceptible to the influence of different situations. In contrast, the disadvantage-averse and equalizing type show relatively low stability in looking patterns across trials, which suggests that their looking behavior is more susceptible to the influence of different situations. The differences in stability of looking patterns between the maximizing and compliant type, and between the disadvantage-averse and the equalizing type, however, were not significant. Taken together, these findings support the interpretation that the maximizing and compliant type show higher capacity for distractor-resistant behavior.

Despite very different distributional preferences, the maximizing and compliant type do not differ regarding their baseline activation in the right IFG and stability in looking patterns. However, these two types differ in their baseline activation in the left OFC: The maximizing type is characterized by higher baseline activation in this area compared to the compliant type. The OFC is part of the so-called brain valuation system (Rangel, Camerer, & Montague, 2008), a neural network involved in the valuation and processing of rewards (e.g., Lopez-Persem et al., 2020; Padoa-Schioppa & Conen, 2017; Zhang, Fanning, et al., 2017; Ruff & Fehr, 2014). We speculate that participants who show increased baseline activation in the left OFC show higher sensitivity for the valuation of rewards and are therefore prone to maximize their outcome. This is also supported by eye-tracking data, that is, the proportion of fixations on distributions, which is a measure of relative importance (Rahal & Fiedler, 2019). Our results show that the maximizing and compliant type inspect the distributions of outcomes and letters very differently, which is in line with the respective decision strategies: The compliant type does not necessarily need to inspect outcomes to find his decisions, whereas the maximizing type only needs to inspect the outcomes. Indeed, we find that whereas the compliant type primarily inspects the letters, the maximizing type primarily inspects the distributions. Hence, the proportion of attention spent on either the outcome or the letter is telling for some behavioral types.

A limitation of this study is that some of the behavioral types were of small size (e.g., equalizing type). This is because of the fact that, unfortunately, we had to stop data acquisition because of the COVID-19 pandemic measures. However, although the size is small in some behavioral types, the effect sizes of the two identified neural signatures (i.e., task-independent baseline activation in the right IFG and left OFC) are not small ($\omega^2 > 0.26$). We therefore believe we are allowed to conclude that our results improve the understanding of different types of distributional preferences. On one hand, the capacity for distractor-resistant behavior is linked to a persons' distributional preference, which is reflected by differences in baseline activation of the right IFG, and to differences in the stability of looking patterns. On the other hand, the sensitivity to react to rewards is reflected by differences in baseline activation of the left OFC and by different weighting of the importance of displayed information. In conclusion, the combination of behavioral measures, source-localized resting EEG, and eye-tracking measures provides novel insights about potential psychological mechanisms associated with differences in distributional preferences.

Reprint requests should be sent to Daria Knoch or Lorena R. R. Gianotti, Department of Social Neuroscience and Social Psychology, Institute of Psychology, University of Bern, Fabrikstrasse 8, CH-3012 Bern, Switzerland, or via e-mail: daria.knoch@psy.unibe.ch, lorena.gianotti@psy.unibe.ch.

Author Contributions

Katharina Koch: Conceptualization; Formal analysis; Investigation; Writing—Original draft. Lorena R. R. Gianotti: Conceptualization; Formal analysis; Funding acquisition; Methodology; Software; Supervision; Writing—Original draft. Jan Hausfeld: Conceptualization; Formal analysis; Investigation; Methodology; Supervision; Writing—Review & editing. Mirjam Studler: Investigation. Daria Knoch: Conceptualization; Funding acquisition; Resources; Supervision; Writing—Review & editing.

Funding Information

Daria Knoch, Swiss National Science Foundation, grant number: 100019_166006. Lorena R. R. Gianotti, Swiss National Science Foundation, grant number: 100019_166006.

Downloaded from http://direct.mit.edu/jocn/article-pdf/33/10/2065/1962120/jocn_a_01751.pdf by guest on 18 October 2021

Diversity in Citation Practices

A retrospective analysis of the citations in every article published in this journal from 2010 to 2020 has revealed a persistent pattern of gender imbalance: Although the proportions of authorship teams (categorized by estimated gender identification of first author/last author) publishing in the *Journal of Cognitive Neuroscience* (*JoCN*) during this period were M(an)/M = .408, W(oman)/M = .335, M/W = .108, and W/W = .149, the comparable proportions for the articles that these authorship teams cited were M/M = .579, W/M = .243, M/W = .102, and W/W = .076 (Fulvio et al., *JoCN*, 33:1, pp. 3–7). Consequently, *JoCN* encourages all authors to consider gender balance explicitly when selecting which articles to cite and gives them the opportunity to report their article's gender citation balance.

REFERENCES

Armbruster, D. J. N., Ueltzhöffer, K., Basten, U., & Fiebach, C. J. (2012). Prefrontal cortical mechanisms underlying individual differences in cognitive flexibility and stability. *Journal of Cognitive Neuroscience*, *24*, 2385–2399. https://doi.org/10.1162/jocn_a_00286, PubMed: 22905818

Ashton, M. C., & Lee, K. (2007). Empirical, theoretical, and practical advantages of the HEXACO model of personality structure. *Personality and Social Psychology Review*, *11*, 150–166. https://doi.org/10.1177/1088868306294907, PubMed: 18453460

Barron, K., Stüber, R., & van Veldhuizen, R. (2019). Motivated motive selection in the lying-dictator game. WZB Discussion Paper (No. SP II 2019-303). Berlin. Retrieved from https://hdl.handle.net/10419/195769.

Baumgartner, T., Gianotti, L. R. R., & Knoch, D. (2013). Who is honest and why: Baseline activation in anterior insula predicts inter-individual differences in deceptive behavior. *Biological Psychology*, *94*, 192–197. https://doi.org/10.1016/j.biopsycho.2013.05.018, PubMed: 23735708

Baumgartner, T., Schiller, B., Hill, C., & Knoch, D. (2013). Impartiality in humans is predicted by brain structure of dorsomedial prefrontal cortex. *Neuroimage*, *81*, 317–324. https://doi.org/10.1016/j.neuroimage.2013.05.047, PubMed: 23689015

Cannon, R. L., Baldwin, D. R., Shaw, T. L., Diloreto, D. J., Phillips, S. M., Scruggs, A. M., et al. (2012). Reliability of quantitative EEG (qEEG) measures and LORETA current source density at 30 days. *Neuroscience Letters*, *518*, 27–31. https://doi.org/10.1016/j.neulet.2012.04.035, PubMed: 22575610

Cappelen, A. W., Hole, A. D., Sørensen, E. Ø., & Tungodden, B. (2007). The pluralism of fairness ideals: An experimental approach. *American Economic Review*, *97*, 818–827. https://doi.org/10.1257/aer.97.3.818

Chapman, L. J., & Chapman, J. P. (1987). The measurement of handedness. *Brain and Cognition*, *6*, 175–183. https://doi.org/10.1016/0278-2626(87)90118-7, PubMed: 3593557

Cohen, T. R., Wolf, S. T., Panter, A. T., & Insko, C. A. (2011). Introducing the GASP scale: A new measure of guilt and shame proneness. *Journal of Personality and Social Psychology*, *100*, 947–966. https://doi.org/10.1037/a0022641, PubMed: 21517196

Cutler, J., & Campbell-Meiklejohn, D. (2019). A comparative fMRI meta-analysis of altruistic and strategic decisions to give. *Neuroimage*, *184*, 227–241. https://doi.org/10.1016/j.neuroimage.2018.09.009, PubMed: 30195947

Dünki, R. M., Schmid, G. B., & Stassen, H. H. (2000). Intraindividual specificity and stability of human EEG: Comparing a linear vs a nonlinear approach. *Methods of Information in Medicine*, *39*, 78–82. https://doi.org/10.1055/s-0038-1634249, PubMed: 10786075

Fiedler, S., Glöckner, A., Nicklisch, A., & Dickert, S. (2013). Social value orientation and information search in social dilemmas: An eye-tracking analysis. *Organizational Behavior and Human Decision Processes*, *120*, 272–284. https://doi.org/10.1016/j.obhdp.2012.07.002

Fischbacher, U. (2007). z-Tree: Zurich toolbox for ready-made economic experiments. *Experimental Economics*, *10*, 171–178. https://doi.org/10.1007/s10683-006-9159-4

Gianotti, L. R. R., Dahinden, F. M., Baumgartner, T., & Knoch, D. (2019). Understanding individual differences in domain-general prosociality: A resting EEG study. *Brain Topography*, *32*, 118–126. https://doi.org/10.1007/s10548-018-0679-y, PubMed: 30267176

Gianotti, L. R. R., Knoch, D., Faber, P. L., Lehmann, D., Pascual-Marqui, R. D., Diezi, C., et al. (2009). Tonic activity level in the right prefrontal cortex predicts individuals' risk taking. *Psychological Science*, *20*, 33–38. https://doi.org/10.1111/j.1467-9280.2008.02260.x, PubMed: 19152538

Gneezy, U., Kajackaite, A., & Sobel, J. (2018). Lying aversion and the size of the lie. *American Economic Review*, *108*, 419–453. https://doi.org/10.1257/aer.20161553

Greiner, B. (2015). Subject pool recruitment procedures: Organizing experiments with ORSEE. *Journal of the Economic Science Association*, *1*, 114–125. https://doi.org/10.1007/s40881-015-0004-4

Hahn, T., Notebaert, K., Anderl, C., Teckentrup, V., Kaßecker, A., & Windmann, S. (2015). How to trust a perfect stranger: Predicting initial trust behavior from resting-state brain-electrical connectivity. *Social Cognitive and Affective Neuroscience*, *10*, 809–813. https://doi.org/10.1093/scan/nsu122, PubMed: 25274577

Hahsler, M., Piekenbrock, M., & Doran, D. (2019). dbscan: Fast density-based clustering with R. *Journal of Statistical Software*, *91*, 1–30. https://doi.org/10.18637/jss.v091.i01

Hsee, C. K., Yang, Y., Zheng, X., & Wang, H. (2015). Lay rationalism: Individual differences in using reason versus feelings to guide decisions. *Journal of Marketing Research*, *52*, 134–146. https://doi.org/10.1509/jmr.13.0532

Jacob, R. J. K., & Karn, K. S. (2003). Eye tracking in human–computer interaction and usability research: Ready to deliver the promises. In J. Hyona, R. Radach, & H. Deubel (Eds.), *The mind's eye: Cognitive and applied aspects of eye movement research* (pp. 573–605). Amsterdam: Elsevier. https://doi.org/10.1016/B978-044451020-4/50031-1

Jiang, T., Potters, J., & Funaki, Y. (2016). Eye-tracking social preferences. *Journal of Behavioral Decision Making*, *29*, 157–168. https://doi.org/10.1002/bdm.1899

Kam, J. W. Y., Bolbecker, A. R., O'Donnell, B. F., Hetrick, W. P., & Brenner, C. A. (2013). Resting state EEG power and coherence abnormalities in bipolar disorder and schizophrenia. *Journal of Psychiatric Research*, *47*, 1893–1901. https://doi.org/10.1016/j.jpsychires.2013.09.009, PubMed: 24090715

Konow, J. (2003). Which is the fairest one of all? A positive analysis of justice theories. *Journal of Economic Literature*, *41*, 1188–1239. https://doi.org/10.1257/002205103771800013

Kubicki, S., Herrmann, W. M., Fichte, K., & Freund, G. (1979). Reflections on the topics: EEG frequency bands and regulation of vigilance. *Pharmakopsychiatrie, Neuro-Psychopharmakologie*, *12*, 237–245. https://doi.org/10.1055/s-0028-1094615, PubMed: 223177

Downloaded from http://direct.mit.edu/jocn/article-pdf/33/10/2065/1962120/jocn_a_01751.pdf by guest on 18 October 2021

Lancaster, J. L., Woldorff, M. G., Parsons, L. M., Liotti, M., Freitas, C. S., Rainey, L., et al. (2000). Automated Talairach atlas labels for functional brain mapping. *Human Brain Mapping*, *10*, 120–131. https://doi.org/10.1002/1097-0193(200007)10:3<120::AID-HBM30>3.0.CO;2-8, PubMed: 10912591

Li, X., Ma, R., Pang, L., Lv, W., Xie, Y., Chen, Y., et al. (2017). Delta coherence in resting-state EEG predicts the reduction in cigarette craving after hypnotic aversion suggestions. *Scientific Reports*, *7*, 2430. https://doi.org/10.1038/s41598-017-01373-4, PubMed: 28546584

Liu, X., Banich, M. T., Jacobson, B. L., & Tanabe, J. L. (2004). Common and distinct neural substrates of attentional control in an integrated Simon and spatial Stroop task as assessed by event-related fMRI. *Neuroimage*, *22*, 1097–1106. https://doi.org/10.1016/j.neuroimage.2004.02.033, PubMed: 15219581

Lopez-Persem, A., Bastin, J., Petton, M., Abitbol, R., Lehongre, K., Adam, C., et al. (2020). Four core properties of the human brain valuation system demonstrated in intracranial signals. *Nature Neuroscience*, *23*, 664–675. https://doi.org/10.1038/s41593-020-0615-9, PubMed: 32284605

Mazziotta, J., Toga, A., Evans, A., Fox, P., Lancaster, J., Zilles, K., et al. (2001). A probabilistic atlas and reference system for the human brain: International Consortium for Brain Mapping (ICBM). *Philosophical Transactions of the Royal Society of London, Series B: Biological Sciences*, *356*, 1293–1322. https://doi.org/10.1098/rstb.2001.0915, PubMed: 11545704

Mobascher, A., Brinkmeyer, J., Warbrick, T., Musso, F., Wittsack, H. J., Saleh, A., et al. (2009a). Laser-evoked potential P2 single-trial amplitudes covary with the fMRI BOLD response in the medial pain system and interconnected subcortical structures. *Neuroimage*, *45*, 917–926. https://doi.org/10.1016/j.neuroimage.2008.12.051, PubMed: 19166948

Mobascher, A., Brinkmeyer, J., Warbrick, T., Musso, F., Wittsack, H. J., Stoermer, R., et al. (2009b). Fluctuations in electrodermal activity reveal variations in single trial brain responses to painful laser stimuli—A fMRI/EEG study. *Neuroimage*, *44*, 1081–1092. https://doi.org/10.1016/j.neuroimage.2008.09.004, PubMed: 18848631

Morishima, Y., Schunk, D., Bruhin, A., Ruff, C. C., & Fehr, E. (2012). Linking brain structure and activation in temporoparietal junction to explain the neurobiology of human altruism. *Neuron*, *75*, 73–79. https://doi.org/10.1016/j.neuron.2012.05.021, PubMed: 22794262

Näpflin, M., Wildi, M., & Sarnthein, J. (2007). Test–retest reliability of resting EEG spectra validates a statistical signature of persons. *Clinical Neurophysiology*, *118*, 2519–2524. https://doi.org/10.1016/j.clinph.2007.07.022, PubMed: 17892969

Nee, D. E., Wager, T. D., & Jonides, J. (2007). Interference resolution: Insights from a meta-analysis of neuroimaging tasks. *Cognitive, Affective, & Behavioral Neuroscience*, *7*, 1–17. https://doi.org/10.3758/CABN.7.1.1, PubMed: 17598730

Nichols, T. E., & Holmes, A. P. (2002). Nonparametric permutation tests for functional neuroimaging: A primer with examples. *Human Brain Mapping*, *15*, 1–25. https://doi.org/10.1002/hbm.1058, PubMed: 11747097

Nuwer, M. R., Comi, G., Emerson, R., Fuglsang-Frederiksen, A., Guérit, J. M., Hinrichs, H., et al. (1998). IFCN standards for digital recording of clinical EEG. International Federation of Clinical Neurophysiology. *Electroencephalography and Clinical Neurophysiology*, *106*, 259–261. https://doi.org/10.1016/S0013-4694(97)00106-5, PubMed: 9743285

Oakes, T. R., Pizzagalli, D. A., Hendrick, A. M., Horras, K. A., Larson, C. L., Abercrombie, H. C., et al. (2004). Functional coupling of simultaneous electrical and metabolic activity in the human brain. *Human Brain Mapping*, *21*, 257–270. https://doi.org/10.1002/hbm.20004, PubMed: 15038007

Orquin, J. L., Ashby, N. J. S., & Clarke, A. D. F. (2016). Areas of interest as a signal detection problem in behavioral eye-tracking research. *Journal of Behavioral Decision Making*, *29*, 103–115. https://doi.org/10.1002/bdm.1867

Orquin, J. L., & Mueller Loose, S. (2013). Attention and choice: A review on eye movements in decision making. *Acta Psychologica*, *144*, 190–206. https://doi.org/10.1016/j.actpsy.2013.06.003, PubMed: 23845447

Padoa-Schioppa, C., & Conen, K. E. (2017). Orbitofrontal cortex: A neural circuit for economic decisions. *Neuron*, *96*, 736–754. https://doi.org/10.1016/j.neuron.2017.09.031, PubMed: 29144973

Pascual-Marqui, R. D. (2002). Standardized low-resolution brain electromagnetic tomography (sLORETA): Technical details. *Methods and Findings in Experimental and Clinical Pharmacology*, *24(Suppl. D)*, 5–12. PubMed: 12575463

Poole, A., Ball, L. J., & Phillips, P. (2005). In search of salience: A response-time and eye-movement analysis of bookmark recognition. In S. Fincher, P. Markopoulos, D. Moore, & R. Ruddle (Eds.), *People and computers XVIII—Design for life* (pp. 363–378). London: Springer-Verlag. https://doi.org/10.1007/1-84628-062-1_23

Rahal, R.-M., & Fiedler, S. (2019). Understanding cognitive and affective mechanisms in social psychology through eye-tracking. *Journal of Experimental Social Psychology*, *85*, 103842. https://doi.org/10.1016/j.jesp.2019.103842

Rangel, A., Camerer, C., & Montague, P. R. (2008). A framework for studying the neurobiology of value-based decision making. *Nature Reviews Neuroscience*, *9*, 545–556. https://doi.org/10.1038/nrn2357, PubMed: 18545266

Ruff, C. C., & Fehr, E. (2014). The neurobiology of rewards and values in social decision making. *Nature Reviews Neuroscience*, *15*, 549–562. https://doi.org/10.1038/nrn3776, PubMed: 24986556

Rullmann, M., Anwander, A., Dannhauer, M., Warfield, S. K., Duffy, F. H., & Wolters, C. H. (2009). EEG source analysis of epileptiform activity using a 1 mm anisotropic hexahedra finite element head model. *Neuroimage*, *44*, 399–410. https://doi.org/10.1016/j.neuroimage.2008.09.009, PubMed: 18848896

Shagass, C. (1972). Electrical activity of the brain. In N. S. Greenfield & R. A. Sternback (Eds.), *Handbook of psychophysiology* (pp. 263–328). New York: Holt, Rinehart, & Winston.

Studer, B., Pedroni, A., & Rieskamp, J. (2013). Predicting risk-taking behavior from prefrontal resting-state activity and personality. *PLoS One*, *8*, e76861. https://doi.org/10.1371/journal.pone.0076861, PubMed: 24116176

Tibshirani, R., Walther, G., & Hastie, T. (2001). Estimating the number of clusters in a data set via the gap statistic. *Journal of the Royal Statistical Society, Series B: Statistical Methodology*, *63*, 411–423. https://doi.org/10.1111/1467-9868.00293

van Velzen, L. S., Vriend, C., de Wit, S. J., & van den Heuvel, O. A. (2014). Response inhibition and interference control in obsessive-compulsive spectrum disorders. *Frontiers in Human Neuroscience*, *8*, 419. https://doi.org/10.3389/fnhum.2014.00419, PubMed: 24966828

Vecchio, F., Babiloni, C., Lizio, R., Fallani, F. D. V., Blinowska, K., Verrienti, G., et al. (2013). Resting state cortical EEG rhythms in Alzheimer's disease: Toward EEG markers for clinical applications: A review. *Supplements to Clinical Neurophysiology*, *62*, 223–236. https://doi.org/10.1016/b978-0-7020-5307-8.00015-6, PubMed: 24053043

Downloaded from http://direct.mit.edu/jocn/article-pdf/33/10/2065/1962120/jocn_a_01751.pdf by guest on 18 October 2021

Watanabe, T., Takezawa, M., Nakawake, Y., Kunimatsu, A., Yamasue, H., Nakamura, M., et al. (2014). Two distinct neural mechanisms underlying indirect reciprocity. *Proceedings of the National Academy of Sciences, U.S.A.*, *111*, 3990–3995. https://doi.org/10.1073/pnas.1318570111, PubMed: 24591599

Zhang, R., Geng, X., & Lee, T. M. C. (2017). Large-scale functional neural network correlates of response inhibition: An fMRI meta-analysis. *Brain Structure & Function*, *222*, 3973–3990. https://doi.org/10.1007/s00429-017-1443-x, PubMed: 28551777

Zhang, Z., Fanning, J., Ehrlich, D. B., Chen, W., Lee, D., & Levy, I. (2017). Distributed neural representation of saliency controlled value and category during anticipation of rewards and punishments. *Nature Communications*, *8*, 1907. https://doi.org/10.1038/s41467-017-02080-4, PubMed: 29203854

Downloaded from http://direct.mit.edu/jocn/article-pdf/33/10/2065/1962120/jocn_a_01751.pdf by guest on 18 October 2021